

Theoretical study of the effective g-factor of Cd_{1-x}Mn_xTe quantum wire under the combined effects of the applied magnetic field, spin-orbit coupling, and exchange effects

Mohammad Elsaid, Diana Dahliah, Ayham Shaer, Mahmoud Ali

Department of Physics, An-Najah National University, Palestine

Corresponding author: Mohammad Elsaid, mkelsaid@najah.edu

ABSTRACT In this paper, the energy formula for charge carrier (e) confined in a diluted magnetic semiconductor (DMS) quantum well QW made from Cd_{1-x}Mn_xTe is generated and utilized to calculate the Density of States (DOS) and the Lande g-factor. The Landau levels in a quantum wire that is placed in uniform magnetic field along its axis, taking into account the presence of Rashba spin-orbit interaction and exchange effect, are explored. These effects have altered the DOS and the Landau levels. The electron g-factor for the lowest state is explored. Our results show that the g-factor is strongly affected by the combined effects of magnetic field and Rashba spin-orbit interaction strengths. The g-factor can vary in a wide range of expands for the bulk value of 2 up to 300, which makes it a good candidate for spintronic applications.

KEYWORDS Lande g-factor, Rashba effect, magnetic field, density of states

ACKNOWLEDGEMENTS This research receives funding from An-Najah National University Grant No. ANNU-2219-Sc0n1

FOR CITATION Elsaid M., Dahliah D., Shaer A., Ali M. Theoretical study of the effective g-factor of Cd_{1-x}Mn_xTe quantum wire under the combined effects of the applied magnetic field, spin-orbit coupling, and exchange effects. *Nanosystems: Phys. Chem. Math.*, 2025, **16** (3), 274–281.

1. Introduction

At the nanoscale, electrons in nanostructures behave differently compared to bulk materials. The two main reasons cause the properties of nanomaterials to significantly deviate from those of bulk materials are the effects of quantum confinement and the increase in the relative surface area to volume ratio. These factors can alter or enhance the properties such as reactivity, as well as the optical, and magnetic characteristics of nanomaterials [1–5]. The optical and electrical characteristics of low-dimensional semiconductor structures such as quantum wires have attracted considerable interest in recent years due to their potential technological applications [6, 7]. The spin-dependent phenomena in quantum wires (QW) have promoted the implementation of these nanowires as potential building blocks in spin electronic devices and future quantum devices [7–9]. Researchers have been exploring nanowires from various materials, well-developed material synthesis, and fabrication techniques have enabled the production of high-quality quantum wires with precise control over their dimensions and properties. For example, chemical precipitation, and laser ablation has been used to produce high-quality nanowires [10, 11].

It has been noticed that the electron spin plays a crucial role in influencing the electrical and optical properties of QW semiconductor structures. Numerous theoretical studies have offered deeper insights into the electrical, dynamical and thermal properties in one-dimensional systems. Kasapoglu et al. studied the combined effects of electric and magnetic fields on the optical absorption coefficients and refractive index changes in GaAs nanowires using the effective-mass approximation and the compact density-matrix approach [12]. A. Bouazra et al. investigated the stability of quantum wire with respect to its shape and size. They examined the optical properties, as well as the energy levels of electrons and holes, along with their corresponding wave functions in various shapes of InAs quantum wires [13]. R. Khordad studied the influence of the external magnetic field and the Rashba effect on the optical properties of 1D quantum wire [14]. Y. Khoshbakht investigated the thermodynamic properties of a nanowire under the presence of the Rashba spin-orbit interaction and external magnetic field. The study provided analytical expressions for the mean energy, the free energy, the specific heat, the entropy, and the magnetic susceptibility of nanowires in the presence of gate-controlled Rashba spin-orbit interaction and an in-plane magnetic field [15]. B. H. Mehdiyev investigated the effect of finite temperature on the electrical conductance of diluted magnetic semiconductor cylinders made of CdTe [16].

One of the essential material parameters of a QW is the effective Lande g-factor. This parameter represents the response of a material to a magnetic field. The study of the effective Lande g-factor in semiconductor nanowires has received great attention because of its importance in manipulating the spin splitting of carrier bands. Its effect on device

performance should be considered. In particular, exploring the g-factor provides a deeper understanding of the behavior of electrons in magnetic fields and helps scientists assist these findings in practical applications.

Many studies have been carried out on the effective Lande g-factor in low-dimensional structures. Several theoretical and experimental studies examine the effect of spin-orbit coupling and the magnetic field on the g-factor. The effects of the magnetic field and Rashba effect on the Lande g-factor in the InAs quantum wire have been examined [17]. In Ref. [18], the authors have explored the g-factor in diluted magnetic semiconductor (DMS) quantum well with parabolic potential in the presence of an external perpendicular magnetic field, the study shows that the g-factor increases with increasing the magnetic field due the increment in the strength of spin-orbit coupling [18]. The authors examined the electron g-factor for various sub-bands in quantum wire in Ref. [19], the effects of electric field, magnetic field, and Rashba spin-orbit interaction strength on g-factor have been explored.

Rogério de Sousa et. al found that the g-factor of a heterojunction quantum dot is very sensitive to its radius and magnetic field arising from the interplay between Rashba and Dresselhaus spin-orbit interactions [20]. Rodrigues et al. investigated the optical properties of CdMnTe/CdTe heterostructures grown on Si substrate, highlighting the effects of quantum confinement and structural roughness on emission spectrum [21].

In this work, we will study the g-factor in Cadmium Telluride material that doped with Manganese Cd_{1-x}Mn_xTe nanowires, where x is the fraction of moles of Mn ions. The spin splitting of the sub-bands can be enhanced by introducing magnetic ions (Mn). The strong s-d exchange interaction between the carriers and the local magnetic ions can be enhanced by an external magnetic field [22, 23]. The Lande g-factor in Cd_{1-x}Mn_xTe nanowires can be controlled by varying the magnetic field, the concentration of Mn, the radius of the wire and it's temperature. It has been recorded that the Lande g-factor in CdTe at zero magnetic field is -0.5 while for Cd_{0.98}Mn_{0.02}Te, it goes to 100 at 4 K [24]. Afanasiev et al. explored the behavior of the electron g-factor due to the s-d exchange interaction between electrons and manganese ions in coupled quantum wells of CdTe and CdMnTe, where the dependence of electron g-factor on the barrier thickness and temperature is experimentally investigated [25].

This work aims to compute and investigate the dependence of energy spectra Density of States (DOS) and effective Lande g-factor of CdMnTe QW. A theoretical examination of the Lande g-factor in a CdMnTe QWs is carried out, considering the effects of an external magnetic field, with particular emphasis on the Rashba effect and the exchange interactions.

2. Theoretical model

The Hamiltonian of an electron in quantum wire (QW) of a given radius ρ under an external magnetic field (B) in the z -direction that is parallel to the axis of the wire that represented the kinetic energy operator term and confinement potential term is given by [18]:

$$H = \frac{-\hbar^2}{2m^*} \left(\frac{1}{\rho^2} \frac{\partial^2}{\partial \varphi^2} + \frac{\partial^2}{\partial z^2} \right) - i\hbar \frac{eB}{2m^*} \frac{\partial}{\partial \varphi} + \frac{e^2 B^2 \rho^2}{8m^*} + \frac{1}{2} g^* \mu_B B \sigma_z + \frac{-1}{2} S_0 B_{5/2} \left(\frac{S g_{Mn} \mu_B B}{K_B (T + T_0)} \right) N_0 x J_{s-d} \sigma_z + \frac{\alpha}{\hbar} [\vec{\sigma} \times \vec{P}] \cdot \vec{n}. \quad (1)$$

Where, in this model, the vector potential induced by the magnetic field is defined as $A = \left(\frac{-By}{2}, \frac{Bx}{2}, 0 \right)$. The constants that are in the Hamiltonian are defined as g^* and m^* donated the electron effective g-factor and effective mass, respectively. σ_z denotes the Pauli spin matrix along the z -axis. The third term represents the Zeeman effect, that will lead to extra energy splitting in the spectrum. The fourth term indicates the exchange effect which describes the s-d exchange Heisenberg interaction between the conduction electrons and Mn ions. Where S_0 is the effective spin, $B_{5/2}$ is the Brillouin function, S is the spin of the localized electrons of Mn ions, g_{Mn} is the g-factor of Mn, k_B is the Boltzmann constant, N_0 is the density of unit cells and J_{s-d} is constant which describe the exchange interaction according to the s-d exchange integral. The last term is the Rashba term which significantly influences the magnetic properties of Mn-doped CdTe wire. Here \vec{P} is the momentum operator, α is the strength of the spin orbit coupling, $\vec{\sigma} = (\sigma_x, \sigma_y, \sigma_z)$ denotes the Pauli spin matrices and \vec{n} is the unit normal to the surface.

After determining each term of the Hamiltonian, the full Hamiltonian is written in a matrix form as follows:

$$\begin{pmatrix} H_{11} - \varepsilon & \alpha e^{i\varphi} \frac{\partial}{\partial z} \\ -\alpha e^{i\varphi} \frac{\partial}{\partial z} & H_{22} - \varepsilon \end{pmatrix} \begin{pmatrix} \psi_1(\varphi, z) \\ \psi_2(\varphi, z) \end{pmatrix}, \quad (2)$$

where,

$$H_{11} = -\frac{\hbar}{2m^*} \left(\frac{1}{\rho^2} \frac{\partial^2}{\partial \varphi^2} + \frac{\partial^2}{\partial z^2} \right) - i\hbar \frac{eB}{2m^*} \frac{\partial}{\partial \varphi} + \frac{e^2 B^2 \rho^2}{8m^*} - \frac{i\alpha}{\rho} \frac{\partial}{\partial \varphi} + \frac{eB\rho}{2\hbar c} \alpha + \frac{1}{2} g^* \mu_B B + 3A,$$

$$H_{22} = -\frac{\hbar}{2m^*} \left(\frac{1}{\rho^2} \frac{\partial^2}{\partial \varphi^2} + \frac{\partial^2}{\partial z^2} \right) - i\hbar \frac{eB}{2m^*} \frac{\partial}{\partial \varphi} + \frac{e^2 B^2 \rho^2}{8m^*} + \frac{i\alpha}{\rho} \frac{\partial}{\partial \varphi} - \frac{eB\rho}{2\hbar c} \alpha - \frac{1}{2} g^* \mu_B B - 3A.$$

A is given by $\frac{1}{6} S_0 B_{5/2} \left(\frac{S g_{Mn} \mu_B B}{K_B (T + T_0)} \right) N_0 x J_{s-d}$, and the wave function is $\psi_n(\varphi, z) = e^{ik_z z} e^{in\varphi} f$ which is the product of plane wave with angular part.

By diagonalizing the Hamiltonian Matrix, the energy dispersion relation for confined electron of the two sub-bands of each index (n) found to be:

$$E_{n\mp} = \frac{\hbar^2(2K^2 - \gamma_1 - \gamma_2 + \gamma_3 + \gamma_4)}{4m\rho^2} \mp \frac{1}{4m\rho} \sqrt{(4mK\alpha)^2 + \hbar^4(\gamma_1 - \gamma_2 - \gamma_3 + \gamma_4)^2}, \quad (3)$$

$$\gamma_3 = n \left(\rho^2 \frac{eB}{\hbar} + \frac{2m\alpha\rho}{\hbar^2} + n \right), \quad (4)$$

$$\gamma_4 = n \left(\rho^2 \frac{eB}{\hbar} - \frac{2m\alpha\rho}{\hbar^2} + n + 1 \right) \quad (5)$$

$$\gamma_1 = -\frac{mg\mu_B B \rho^2}{\hbar^3} - \frac{6Am\rho^2}{\hbar^2} + \left(-\frac{\alpha m \rho^3}{\hbar^2} - \frac{\rho^4}{4} \right) \frac{eB}{\hbar} \quad (6)$$

$$\gamma_2 = \frac{mg\mu_B B \rho^2}{\hbar^3} + \frac{6Am\rho^2}{\hbar^2} + \left(\frac{\alpha m \rho^3}{\hbar^2} - \frac{\rho^4}{4} \right) \frac{eB}{\hbar}. \quad (7)$$

The energy in Eq. (3) depends on the radius of the nanowire, the strength of the external magnetic field, the Rashba parameter, the magnetic ion concentrations and the temperature.

The energy dispersion relation is used to calculate the density of states DOS of the electrons in the CdTe QW. The DOS is defined mathematically as the delta function and it can be written in terms of Green's function as follows

$$\text{DOS}(E) = -\frac{1}{\pi} \sum_E \text{Im}(G(E, \epsilon)), \quad (8)$$

where E is the energy, and ϵ is a very small parameter. Green's function is defined as:

$$G(E, \epsilon) = \frac{1}{H - E + i\epsilon}. \quad (9)$$

In addition to previous quantities, the effective Lande g-factor (g) is computed for the low-lying state using the relation

$$g = \frac{E_0(\uparrow) - E_0(\downarrow)}{\mu_B B}. \quad (10)$$

3. Results and discussions

In this section, we present the computed results for Landau energies of an electron confined in a cylindrical quantum wire under the presence of an external magnetic field, for different ranges of physical parameters. In the following computations, the values of the parameters in the energy expression are as follows: $S = 5/2$ corresponding to the spins of the localized electrons of Mn ions, the g-factor of Mn $g_{Mn} = 2$, the effective spin $S_0 = 1.97$, $T_0 = 3K$, $m^* = 0.096m_e$, $J_{s-d} = 220$ meV, and $g^* = -1.47$. These values are taken from the literature [26].

In Fig. 1, the eigenenergies of different states range from $n = -2$ to $n = 2$ are plotted against the applied magnetic field for (a) in the presence of Rashba effect and (b) in the presence of Rashba and exchange effects for the two sublevels of each state: (spin up: solid line, and spin down: dotted line). The plot shows that the magnitude of the energy increases with increasing the external magnetic field, this can be explained as the increment of the magnetic field will enhance the confinement potential on the electron, so the energy splitting will be increased as it is expected.

The effect of the Rashba parameter (α) on the eigenenergies has been taken into account, Fig. 1(a) shows the enactment in the Rashba constant α from 50 to 100 meV·nm changes the magnitude of the energy levels (red for $\alpha = 50$ meV·nm and blue for 100 meV·nm), Rashba effect shifts the energy of the states with spin down to higher energy values, while shifting the energy of spin-up states to less positively energy under given value of the magnetic field. In Fig. 1(b), we show the exchange effect, in the presence of the Rashba effect, the exchange term has different influence on shifting the energy of the sublevels in the presence of the magnetic field compared to the Rashba term. By enhancing the exchange interaction through an increase in Mn ions, the spin-down states shift to lower energy levels, while the spin-up states move to higher energy levels. The energy change is due to the exchange term in the Hamiltonian being linearly proportional to the number of Mn ions in the CdTe nanowire. Furthermore, Fig. 1 demonstrates that the crossing point (degeneracy point) between the sublevels of the ground state shifts to higher magnetic field values as the molar concentration of Mn is increased. With increasing the magnetic field, energy levels corresponding to different quantum numbers (different sub bands). When such a crossing occurs, the ground state can switch to a different quantum number.

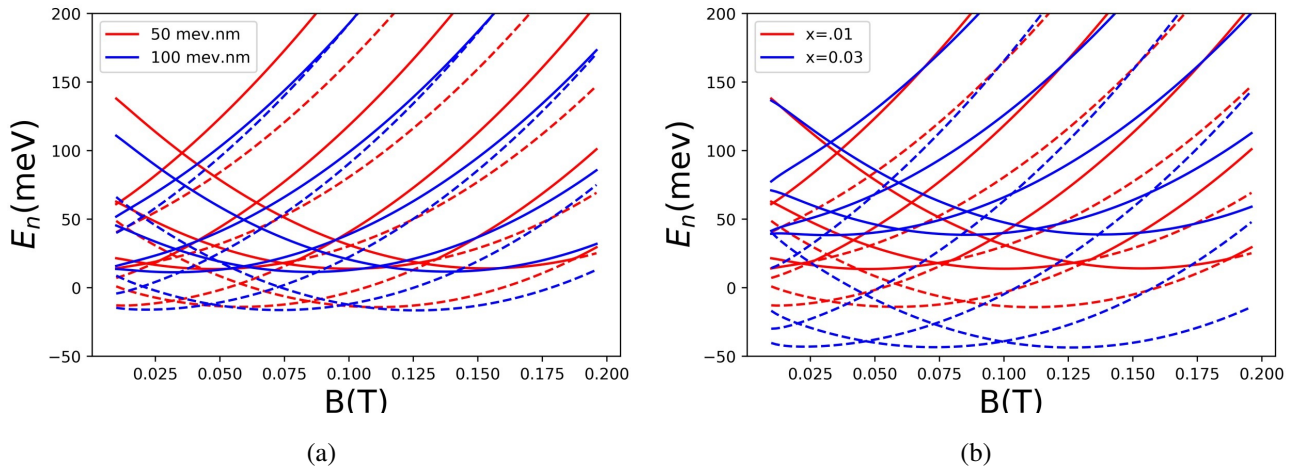


FIG. 1. The low-lying energy of states as a function of magnetic field (spin-up states in solid lines while spin-down in dashed lines) (a) in the presence of spin-orbit interaction only (red: $\alpha = 50 \text{ meV}\cdot\text{nm}$, blue: $100=50 \text{ meV}\cdot\text{nm}$) (b) In the presence of the combined effect of RSOI and exchange effects (red: $x = 0.01$, $x = 0.03$)

The density of states $DOS(E)$, which represents the number of states per unit of energy, is a fundamental property in solid-state physics and condensed matter. It is used to study electronic structure and carrier concentration, which, in turn, determine the type of matter and its conductivity. Therefore, we highlight the effects of Rashba and the exchange term on the density of the states of electrons.

Figure 2 displays the density of states DOS as a function of energy. Fig. 2(a) represents the density of states of spin up and spin down as a function of energy for $Cd_{0.98}Mn_{0.02}Te$ of radius 10 nm in the presence of an external magnetic field of 1 T taken into account the Rashba effect of ($\alpha = 50 \text{ meV}\cdot\text{nm}$). The presence of the Rashba spin orbit interaction lifts the degeneracy in the states, and as it can be noticed the number of states is more at low energy values. The Rashba spin orbit interaction reduces the difference in energy between the spin up and the spin down states as can be seen in Fig. 2(a). Also, it can be noticed at a given value of energy, it is more preferred to occupy the spin-up state compared to the spin-down state as the spin-up state has lower energy compared to the spin-down state. It's evident from the comparison between Fig. 2(a and b) after enhancing the exchange effect, by increasing x from 0.02 to 0.04, the degeneracy between the states are removed. By making a comparison between Fig. 2(a and b), it can be noticed that the separation in DOS peaks for the spin down levels is much larger compared to spin up.

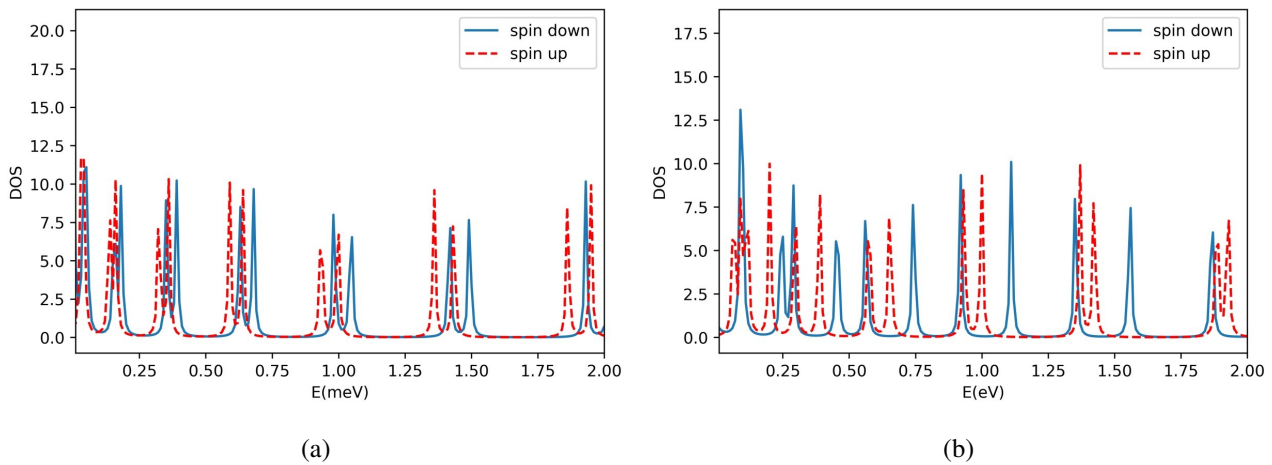


FIG. 2. The density of states of spin up and spin down as a function of energy for (a) $Cd_{0.98}Mn_{0.02}Te$ (b) $Cd_{0.96}Mn_{0.04}Te$ QW of radius 10nm in the presence of an external magnetic field of 1 T

The effective Lande g -factor of the electron in quantum wire made from CdMnTe (QW) under an external magnetic field (B) in the z -direction that is parallel to the axis as a function of the radius of the confinement ρ , magnetic field (B), the Rashba parameter (α), Mn ions concentration (x), and temperature (T) is examined.

In Fig. 3, the effective Lande g -factor has been plotted as a function of the QW radius for Cd_{0.99}Mn_{0.01}Te in the presence of an external magnetic field of 1 T taking into account the Rashba spin orbit interaction ($\alpha = 50$ meV·nm). From Fig. 3, it is clear that as the radius of the confinement increases the g -factor decreases, and it reaches its bulk value for large values of ρ . It can be noticed that by modulating the radius of the QW, the g -factor can be tuned in a range from 2 to 200 which makes it a suitable for a wide range of applications. However, for experimental implementation, other factors should be considered, particularly, strain effects. Additional factors such as structural disorder, interfaces, and lattice strain can influence the effective g -factor. Disorder and impurity scattering may cause a modifying in the spin splitting effects induced by the Rashba spin-orbit interaction and exchange coupling. Similarly, strain in the crystal lattice can lift band degeneracies and alter the spin-orbit coupling strength, thereby affecting the g -factor. While these effects are beyond the scope of the present analytical model, they are crucial in realistic systems and should be taken into account when interpreting experimental data or designing spintronic devices based on Mn-doped CdTe nanostructures.

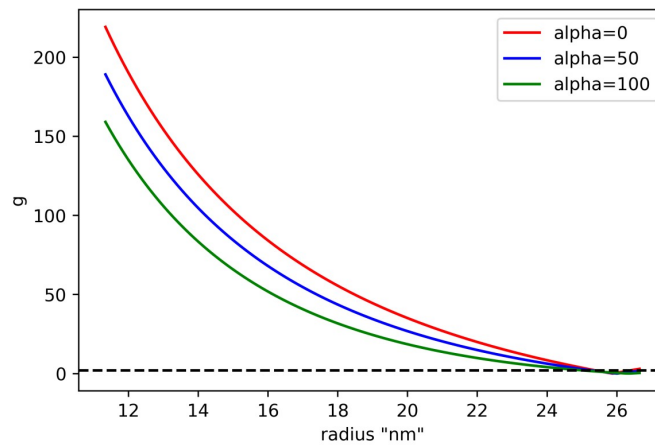


FIG. 3. The effective Lande g -factor vs. QW radius of for Cd_{0.99}Mn_{0.01}Te in the presence of an external magnetic field of 1 T

In Fig. 4, the effective Lande g -factor has been plotted as a function of the magnetic field (B) for Cd_{0.98}Mn_{0.02}Te of radius 30nm in the presence of external magnetic field taken into account the Rashba effect (α ranges from 50 up to 150 meV·nm). In CdTe QWs, in the absence of Rashba spin-orbit interaction, the effective g -factor increases with the applied magnetic field. This increase is attributed to the enhancement of the carrier confinement potential induced by the magnetic field. However, this confinement-induced enhancement of the g -factor saturates beyond a magnetic field strength of approximately 3 T. This trend is consistent with previous theoretical and experimental studies [23]. When the Rashba SOI is introduced, the g -factor exhibits a decreasing trend with increasing Rashba coupling strength (α), due to the reduced spin splitting, as illustrated in Fig. 1. The influence of Rashba SOI is particularly prominent at low magnetic fields. For instance, at $\alpha = 50$ meV·nm, the SOI dominates for magnetic fields below 0.4 T, resulting in a decrease in the g -factor as the magnetic field increases. Above 0.4 T, the magnetic confinement becomes the dominant factor, leading to an increase in the g -factor. This behavior is clearly observed for $\alpha = 50$ meV·nm and $\alpha = 100$ meV·nm, as shown in Fig. 4.

For fixed parameters, $\rho = 30$ nm, $B = 1$ T, the SOI can be manipulated by changing the value of α . The SOI strength effect on the Lande g -factor has been investigated in Fig. 5. In the first case, where the exchange interaction is neglected, a QW composed of CdTe is considered (represented by the red line). The effective g -factor decreases with increasing Rashba spin-orbit coupling strength (α). This behavior arises from the enhanced spin-orbit interaction, which reduces the energy splitting between the spin-up and spin-down states of the ground subband, thereby leading to a lower g -factor. However, when the exchange interaction is included the behavior of the g -factor changes. For small Mn concentrations, at low values of α , the Rashba SOI and the exchange interaction act in opposition regarding the spin splitting of the ground state. As a result, increasing α initially reduces the g -factor, reaching a minimum where the opposing effects remove the splitting and lead to a degenerate ground state, leading to an effective g -factor close to zero. Beyond this critical value of α , the Rashba SOI becomes dominant, and both interactions contribute constructively to the spin splitting, resulting in an increase in the g -factor with further increases in α , as illustrated in Fig. 5. In the case of stronger exchange interaction (e.g., higher Mn concentration, represented by the black line), the exchange term dominates. Here, the g -factor increases with increasing α . This behavior is evident for Mn concentrations of $x = 0.01$ and $x = 0.05$. The observed increase

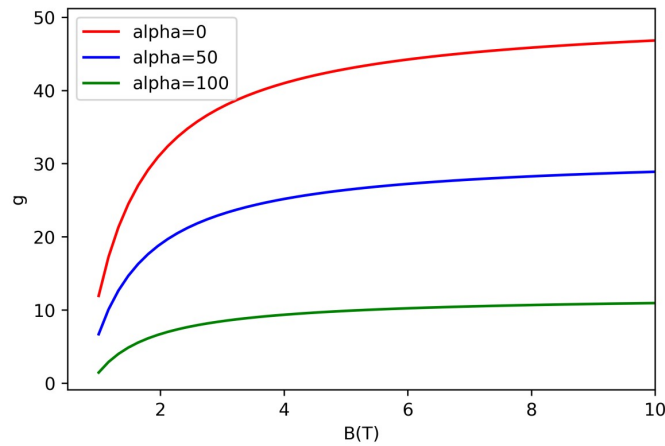


FIG. 4. Effective Lande g-factor vs. magnetic fields for CdTe QW at different values of the Rashba parameter ($\alpha = (0.50 \text{ and } 100 \text{ meV}\cdot\text{nm})$)

in g-factor can be explained by the exchange interaction, which enhances the energy splitting between spin-up and spin-down states in the ground subband as the Mn ion concentration increases. Since the g-factor is directly proportional to this energy splitting, it increases accordingly.

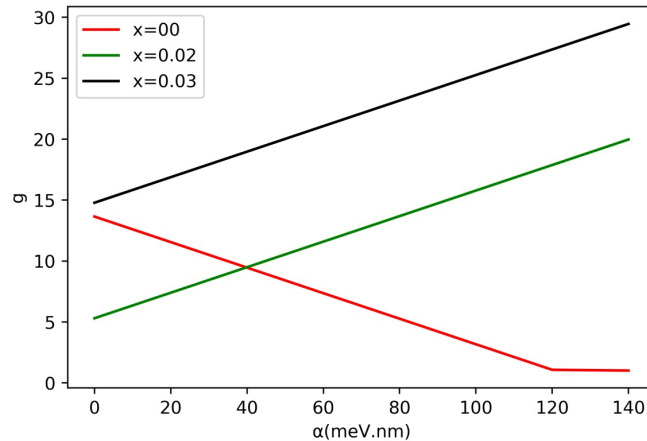


FIG. 5. Effective Lande g-factor vs. Rashba coefficient (α)

The influence of exchange interaction is also investigated. Fig. 6 illustrates the dependence of the effective g-factor on the Mn ion concentration (x) at various temperatures below 20 K. For a fixed temperature, the g-factor initially decreases with increasing Mn molar concentration in the low- x regime. This decrease is attributed to the dominance of the Rashba SOI, which suppresses the spin splitting. As x increases further, the g-factor reaches a minimum (critical value) and subsequently increases approximately linearly with increasing x , due to the growing dominance of the exchange interaction, as discussed earlier.

As temperature increases, the g-factor decreases for a given Mn concentration. This reduction is due to the thermal fluctuations of magnetic moments, which weakens their alignment with the external magnetic field and thus diminishes the strength of the exchange interaction. As a consequence, the critical Mn concentration at which the g-factor begins to increase shifts to higher values with increasing temperature. This temperature dependence is further illustrated in Fig. 7. As shown, higher temperatures reduce the g-factor, and at elevated temperatures, the g-factor tends to approach its bulk semiconductor value. This behavior is consistent with the temperature dependence of the Brillouin function, which governs the magnetization of Mn ions and decreases with increasing temperature. As a result, the exchange-induced energy splitting between spin-up and spin-down states diminishes at higher temperatures, leading to a reduction in the effective g-factor.

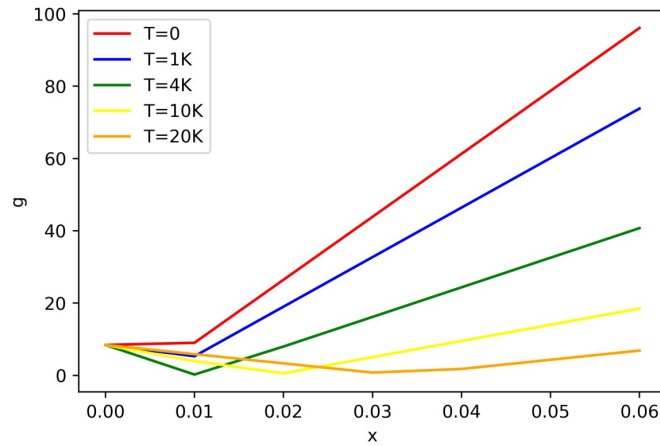


FIG. 6. Effective Lande g-factor vs. Mn molar concentration (x)

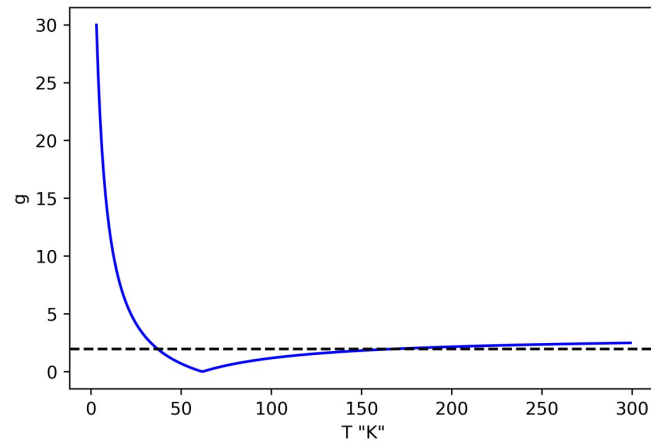


FIG. 7. The effective Lande g-factor vs. Temperature of for $\text{Cd}_{0.99}\text{Mn}_{0.01}\text{Te}$ in the presence of an external magnetic field of 1 T

4. Conclusion

In this work, we have analytically studied the energy spectrum of a cylindrical quantum wire (QW) composed of CdTe under an external magnetic field, incorporating both Rashba spin-orbit interaction (SOI) and exchange interaction effects. These interactions significantly influence the density of states (DOS) and modify the Landau level structure. We focused particularly on the behavior of the electron effective g-factor associated with the zeroth Landau level, demonstrating its strong dependence on both the magnetic field strength and the Rashba SOI parameter.

Our results reveal that, in Mn-doped CdTe quantum wires, the effective g-factor increases with the strength of the Rashba SOI, especially when the exchange interaction becomes significant. By tuning structural parameters of the QW and the Mn ion concentration, it is possible to engineer large, tunable g-factors. This tunability opens promising avenues for the use of such nanostructures in spintronic applications, where control over spin-dependent properties is essential.

References

- [1] Zarkevich N.A., Zverev V.I. Viable materials with a giant magnetocaloric effect. *Crystals*, 2020, **10** (9), 815.
- [2] Ali A.A., Shaer A., Elsaid M. Simultaneous effects of Rashba, magnetic field and impurity on the magnetization and magnetic susceptibility of a GaAs-semiconductor quantum ring. *J. of Magnetism and Magnetic Materials*, 2022, **556**, 169435.
- [3] Xiang G., Wang Y.G. Exploring electronic-level principles how size reduction enhances nanomaterial surface reactivity through experimental probing and mathematical modeling. *Nano Research*, 2022, **15**, P. 3812–3817.
- [4] Shaer A., Elsaid M.K. The Gaussian impurity effect on the electronic and magnetic properties of an electron confined in a lateral quantum dot. *Nanosystems: Phys., Chem., Math.*, 2022, **13** (3), P. 265–273.
- [5] Shaer A., Yücel M.B., Kasapoglu E. Hydrostatic pressure and temperature dependent optical properties of double inverse parabolic quantum well under the magnetic field. *Physica B: Condensed Matter*, 2024, **685**, 416057.

- [6] Tsovolikos A., Jariwala A., Suryanarayanan S., Bakolas E., Goldstein D. Separation delay in turbulent boundary layers via model predictive control of large-scale motions. *Physics of Fluids*, 2023, **35** (11), 115118.
- [7] Evseev S.S., Burmistrov I.S., Tikhonov K.S., Kachorovskii V.Y. Effect of elastic disorder on single-electron transport through a buckled nanotube. *Physical Review Research*, 2022, **4** (1), 013068.
- [8] Kim W.Y., Choi Y.C., Kim K.S. Understanding structures and electronic/spintronic properties of single molecules, nanowires, nanotubes, and nanoribbons towards the design of nanodevices. *J. of Materials Chemistry*, 2008, **18** (38), P. 4510–4521.
- [9] Zeng Z., Zhou C., Zhou H., et al. Spectral evidence for Dirac spinons in a kagome lattice antiferromagnet. *Nature Physics*, 2024, **20**, P. 1097–1102.
- [10] Xiao J., Liu P., Wang C.X., Yang G.W. External field-assisted laser ablation in liquid: An efficient strategy for nanocrystal synthesis and nanostructure assembly. *Progress in Materials Science*, 2017, **87**, P. 140–220.
- [11] Elsbahy M., Heo G.S., Lim S.M., Sun G., Wooley K.L. Polymeric nanostructures for imaging and therapy. *Chemical reviews*, 2015, **115** (19), P. 10967–11011.
- [12] Kasapoglu E., Urgan F., Duque C.A., Yesilgul U., Mora-Ramos M.E., Sar H., So I. The effects of the electric and magnetic fields on the nonlinear optical properties in the step-like asymmetric quantum well. *Physica E: Low-dimensional Systems and Nanostructures*, 2014, **61**, P. 107–110.
- [13] Bouazra A., Nasrallah S.A.B., Said M. Theory of electronic and optical properties for different shapes of InAs/InO. 52AlO. 48As quantum wires. *Physica E: Low-dimensional Systems and Nanostructures*, 2016, **75**, P. 272–279.
- [14] Khordad R. Optical properties of quantum wires: Rashba effect and external magnetic field. *J. of luminescence*, 2013, **134**, P. 201–207.
- [15] Khoshbakht Y., Khordad R., Rastegar Sedehi H.R. Magnetic and thermodynamic properties of a nanowire with Rashba spin–orbit interaction. *J. of Low Temperature Physics*, 2021, **202**, P. 59–70.
- [16] Mehdiyev B.H., Babayev A.M., Cakmak S., Artunc E. Rashba spin–orbit coupling effect on a diluted magnetic semiconductor cylinder surface and ballistic transport. *Superlattices and Microstructures*, 2009, **46** (4), P. 593–602.
- [17] Gharaati A., Khordad R. Electron g-factor in quantum wire in the presence of Rashba effect and magnetic field. *Superlattices and Microstructures*, 2012, **51** (1), P. 194–202.
- [18] Babanlı A.M., Artunç E., Kasalak T.F. Electron g-Factor in Diluted Magnetic Semiconductor Quantum Well with Parabolic Potential in the Presence of Rashba Effect and Magnetic Field. *Zeitschrift für Naturforschung A*, 2015, **70** (2), P. 109–114.
- [19] Kumar M., Lahon S., Jha P.K., Mohan M. Energy dispersion and electron g-factor of quantum wire in external electric and magnetic fields with Rashba spin orbit interaction. *Superlattices and Microstructures*, 2013, **57**, P. 11–18.
- [20] De Sousa R., Sarma S.D. Gate control of spin dynamics in III-V semiconductor quantum dots. *Physical Review B*, 2003, **68** (15), 155330.
- [21] Rodrigues L.N., Inoch W.F., Gomes M.L.F., Couto Jr.O.D.D., Archanjo B.S., Ferreira S.O. Localized-states quantum confinement induced by roughness in CdMnTe/CdTe heterostructures grown on Si(111) substrates. *J. of Semiconductors*, 2024, **45** (9), 092301.
- [22] Furdyna J.K. Diluted magnetic semiconductors. *J. of Applied Physics*, 1988, **64** (4), R29–R64.
- [23] Jin H., Livache C., Kim W.D., Diroll B.T., Schaller R.D., Klimov V.I. Spin-exchange carrier multiplication in manganese-doped colloidal quantum dots. *Nature materials*, 2023, **22** (8), P. 1013–1021.
- [24] Brandt N.B., Moshchalkov V.V. Semimagnetic semiconductors. *Advances in Physics*, 1984, **33** (3), P. 193–256.
- [25] Afanasiev M.M., Kozyrev N.V., Kirstein E., Kalevich V.K., Zhukov E.A., Mantsevich V.N., Krivenko I.S., Karczewski G., Yakovlev D.R., Kusraev Yu.G., Bayer M. Electron g-factor in coupled quantum wells CdTe and CdMnTe. *J. of Physics: Conference Series*, 2019, **1400** (6), 066023.
- [26] Kirstein E., Kozyrev N.V., Afanasiev M.M., Mantsevich V.N., Krivenko I.S., Kalevich V.K., Bayer M. Short range proximity effect induced by exchange interaction in tunnel-coupled CdTe and (Cd, Mn) Te quantum wells. *Physical Review B*, 2020, **101** (3), 035301.

Submitted 21 October 2024; revised 24 April 2025; accepted 8 May 2025

Information about the authors:

Mohammad Elsaid – Department of Physics, An-Najah National University, Palestine; ORCID 0000-0002-1392-3192; mkelsaid@najah.edu

Diana Dahliah – Department of Physics, An-Najah National University, Palestine; ORCID 0000-0002-6919-3539; diana.dahliah@najah.edu

Ayham Shaer – Department of Physics, An-Najah National University, Palestine; ORCID 0000-0002-6518-6470; ayham.shaer@najah.edu

Mahmoud Ali – Department of Physics, An-Najah National University, Palestine; ORCID 0000-0002-3738-5851; mahmoud.ali@najah.edu

Conflict of interest: the authors declare no conflict of interest.